Toward Autonomous Pulmonary Artery Catheterization: A Learning-based Robotic Navigation System

Yaxi Wang[1], Vivek Muthurangu[2] and Helge A Wurdemann[1]

***Abstract*— Providing imaging during interventional treatments of cardiovascular diseases is challenging. Magnetic Resonance Imaging (MRI) has gained popularity as it is radiation-free and returns high resolution of soft tissue. However, the clinician has limited access to the patient, e.g., to their femoral artery, within the MRI scanner to accurately guide and manipulate an MR-compatible catheter. At the same time, communication will need to be maintained with a clinician, located in a separate control room, to provide the most appropriate image to the screen inside the MRI room. Hence, there is scope to explore the feasibility of how autonomous catheterization robots could support the steering of catheters along trajectories inside complex vessel anatomies.**

In this paper, we present a Learning from Demonstration based Gaussian Mixture Model for a robot trajectory optimisation during pulmonary artery catheterization. The optimisation algorithm is integrated into a 2 Degree-of-Freedom MR-compatible interventional robot allowing for continuous and simultaneous translation and rotation. Our methodology achieves autonomous navigation of the catheter tip from the inferior vena cava, through the right atrium and the right ventricle into the pulmonary artery where an interventions is performed. Our results show that our MR-compatible robot can follow an advancement trajectory generated by our Learning from Demonstration algorithm. Looking at the overall duration of the intervention, it can be concluded that procedures performed by the robot (teleoperated or autonomously) required significantly less time compared to manual hand-held procedures.

I. Introduction

Cardiovascular diseases (CVDs) are currently responsible for approximately 19.1 million deaths worldwide each year, accounting for approximately 32% of global deaths [1]. CVDs have become the leading cause of death worldwide, including arrhythmias, aortic aneurysms and coronary artery diseases [1]. Cardiac catheterization is becoming increasingly important in the diagnosis and treatment of CVD. During catheterization, a thin tube is inserted into the patient's vasculature using some form of vascular access e.g., through a sheath in the femoral artery or vein [2]. A vital aspect of catheterization is visual feedback, conventionally obtained by X-ray fluoroscopy, which is required to steer and guide the catheter tip to the target position [3].

 This work is supported by the Royal Free Hospital, London, UK, the UCL Dean's Prize, UCL Mechanical Engineering, and the China Scholarship Council (CSC).

[1]Yaxi Wang and Helge A. Wurdemann are with the Department of Mechanical Engineering, University College London, UK. h.wurdemann@ucl.ac.uk. h.wurdemann@ucl.ac.uk

[2]Vivek Muthurangu is with the Institute of Cardiovascular Science, University College London, London, UK v.muthurangu@ucl.ac.uk

Though X-ray based cardiac catheterization is ubiquitous, this imaging modality exposes both patients and clinicians to ionizing radiation, resulting in a significant cancer risk. In addition, X-ray provides poor soft tissue contrast that can make some procedures more difficult. The last 20 years has seen Magnetic Resonance Imaging (MRI) becoming increasingly used for real-time guidance for medical interventions, as it provides high quality radiation free images. This includes MR guided cardiac catheterization, which is now a clinical routine in some centers. However, there are some disadvantages of MRI, particularly the limited access to the patient, which makes catheter manipulation more difficult [5]. To overcome this challenge, as well as the difficult communication in the MRI environment, teleoperated robotic systems have been developed. For instance, Kundrat et al. designed an MR-compatible pneumatic endovascular robotic manipulation platform that mimics the clinician's movements for translation and rotation of an Electrophysiology (EP) catheter. This platform provides intravascular haptic feedback [6], an important aspect clinical catheterization. Tavallaei et al. proposed a 2-Degree-of-Freedom (DoF) MR-compatible catheter navigation system for cardiac catheterization based on USMs, with a master-slave structure designed to allow accurate catheter navigation [7], [8].

Automation has been introduced for interventional and surgical robotic devices with the aim for the robot to execute tasks autonomously [9]. For instance, Calinon et al. proposed a machine learning framework for extracting relevant features for task presentation, using Gaussian Mixture Models (GMM) and its regression and enabling the computation of optimal trajectories for surgical tasks [10]. Tsai et al. designed a robot for autonomous operation for suturing in a restricted space, enabling autonomous surgery through algorithms from human-robot interaction and reinforcement learning [11], [12]. Another example includes the work by Chi et al., who applied reinforcement learning and GMM to a catheterization robot and achieved trajectory optimisation for aortic interventions, improving the success and stability of the operation and reducing the risk of perforation during the procedure [13], [14]. For cardiac catheterization, introducing robotic autonomy may benefit navigation through the complex vascular geometry in terms of safety, procedure time, resource utilization [15]. Reinforcement Machine Learning (RL) has been successfully applied to complex tasks in dynamic environments enabling robots to learn by imitation based on demonstrations [16], [17]. For instance, RL has been implemented in a minimally invasive surgical robotic systems with 4 DoFs for remote trajectory optimisation

and navigation of catheters for cardiac electrophysiological interventions [18]. Research on trajectory optimisation for aortic interventions and EP catheterization has significantly progressed through the application of RL [19], [20]. There is however scope to further explore the feasibility of other automation algorithms for catheterizations [21], [22]. Learning from demonstration has great potential to achieve autonomous catheter advancement [23], [24], [25].

In this paper, we present a Learning from Demonstration (LfD) based Gaussian Mixture Model (GMM) for a robot trajectory optimisation during right heart catheterization. The optimisation algorithm is integrated into a 2-Degree-of-Freedom (DoF) MR-compatible interventional robot allowing for continuous and simultaneous translation and rotation. Our meth achieves autonomous navigation of the catheter tip from the inferior vena cava (IVC), through the right atrium (RA) and the right ventricle (RV) into the pulmonary artery (PA) where pressure measurements are conventionally made.

The remaining paper is organised as follows: An overview of the interventional robotic system with the catheter tip tracking is presented in Section II. In Section III, data acquisition of the catheter tip trajectories are carried out. The data is used for a LfD based GMM for the optimisation and validation of catheter tip trajectories. Section IV and V summarise the discussion and conclusion.

II. Overview of the Interventional Robotic System with Catheter Tip Tracking

A. Compact 2-DoF interventional robot design

For robotic right heart catheterization to be conducted inside an MRI scanner, a 2 DoF MR-compatible interventional robot has been developed (see CAD drawing in Fig. 1). Two piezoelectric ultrasonic motors (USMs) by Tekceleo, France are used to allow continuous rotational and translational motion (see Fig. 1(a)). These USMs are MR-compatible and suitable to operate safely in an MRI scanner. The structure is made of 3D printed resin material (Draft Resin, Formlabs) with an overall dimension of $130x90x115\,\mathrm{mm}^3$. Fig. 1 (b) shows how a catheter can be clamped between two rollers (the master and slave rollers) to then achieve translational movements of the catheter through rotation of the ultrasonic motor (WLG-30). A layer of silicone material (Ecoflex 00-50, $2\,\mathrm{mm}$)) surrounds the master roller to prevent the catheter from being crimped by the rigid structure when being clamped and to increase the friction between the rollers and catheter, hence, transmitting motion. A groove in the centre of the rollers provides guidance for the catheter, thus avoiding deflections or any misalignment during translation. Rotational motion of the catheter is achieved using the second USM (WLG-75) transferring the rotational motion to the central axis of the catheter through a gearing system. The translational section remains clamped to the catheter so that rotation and translation can happen simultaneously. From Fig. 1, it can also be seen that an MR-compatible slip ring is integrated to ensure seamless transmission of power and control signals to the rotating structure of the robot. Manual input to the two USMs can be given via a joystick.

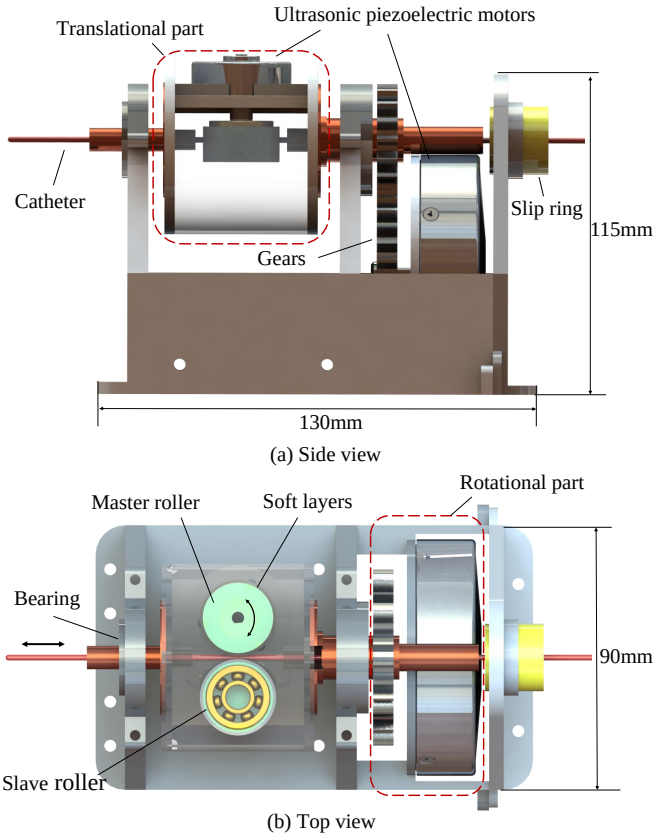

Fig. 1. (a) Side view and (b) top view of our 2-DoF MR-compatible robotic manipulator for pulmonary artery catheterization (PAC). The system is made of two piezoelectric ultrasonic motors (USMs) allowing translational and rotational motion of the catheter.

B. Catheter tip tracking platform inside a phantom

In order to achieve both manual and robotic manipulation of the catheter into the target position of the pulmonary artery phantom, a robotic manipulation platform for catheterization is designed as shown in Fig. 2. Two joystick interfaces enable the remote control of the 2-DOF interventional robot achieving simultaneous translational and rotational movement of the catheter. A 5-DoF tracker is mounted to the tip of the catheter allowing for monitoring and recording real-time position and orientation ($P = (t,\, T_x,\, T_y,\, T_z,\, R_x,\, R_y)$) of the tip for our learning algorithm. The tracking sensor is connected to a magnetic field generator (Aurora, NDI, Canada). The pulmonary artery phantom is made of 3D printed material Vero Clear using a PolyJet Objet 500 Connex. The phantom includes the inferior vena cava (IVC), right atrium (RA), right ventricle (RV) and pulmonary artery (PA). A USB camera captures the movement of the catheter from a top view inside the phantom environment.

III. LfD-based GMM and Experimental Results

A. Methodology

The LfD-based GMM for robot trajectory optimization is divided into four parts [26], [27]:

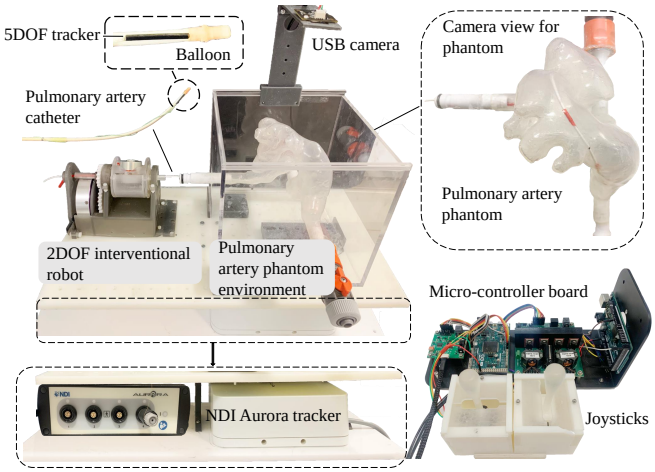

Fig. 2. Interventional robotic platform and phantom environment for pulmonary artery catheterization. Through a joystick interface, the 2-DoF robot advances the catheter inside the pulmonary artery. The catheter is equipped with a 5-DoF magnetic tracker connected to an NDI Aurora tracking system. A USB camera monitors the phantom environment from a top view as shown in the top right figure.

- Collecting position and rotation data sets from demonstration. In this step, the trajectory data of the demonstrated catheter tip is obtained by means of the NDI electromagnetic tracking sensor (see Section III-B).
- Learning and training of the GMM from the trajectory data. The catheter tip trajectory data set is imported into the GMM for training and learning to estimate its probability density distribution (see Section III-C).
- Generating a smoothed trajectory for the interventional robot. The trained GMM dataset is processed by the Gaussian Mixture Regression (GMR) to generate an optimal trajectory of the catheter tip based on LfD (see Section III-C).
- Operating the robot advancing and pulling back the catheter along the optimised trajectory, then comparing with other modes of operation (see Section III-D).

B. Data collection for trajectory optimisation

Manual hand-held catheterization procedures inside the phantom environment were performed including the advancement and pullback of the catheter starting from the IVC, through the RA and RV into the PA and vice versa. The catheter tip position and rotation information of 50 repetitions have been collected by the electromagnetic position sensor with a sampling frequency of 40 HZ. The recorded trajectory dataset was then imported into the GMM.

Robot-assisted catheterization involved an operator using the joystick interface to control the advancement and pullback of the catheter tip inside the phantom environment using the robot (as shown in Fig.1). The same trajectories has been followed as during the manual procedure, starting from the IVC, through the RA and RV into the PA. Again, the time-dependent position and rotation of the catheter tip has been recorded for 50 repetitions have been recorded. In addition, the USB camera in Fig.2 observed the movement of the catheter position information in real-time.

The results from the catheter tip tracking experiments are shown in Figs. 3(a)-(c). In particular, Fig. 3(a) illustrates the trajectories of the catheter tip advancements in the $x-y$ (top) and $x-z$ (bottom) planes. For the catheter pullback procedure, the trajectories are plotted in Fig. 3(b) in the $x-y$ (top) and $x-z$ (bottom) planes. Fig. 3(c) shows a 3D visualisation of the catheter advancement (top) and pullback (bottom) trajectories inside a 3D CAD model of the pulmonary artery phantom. The trajectories for the catheter advancements and pullbacks are distinguishable as the trajectories for the advancements are more distributed among the inner volume of the phantom. The larger distribution results from the challenging task to steer the catheter along the complex anatomy starting from the IVC, through the RA and RV into the PA. In comparison, pulling back the catheter does not involve navigation but extracting the medical device.

C. LfD-based GMM

Time-dependent catheter tip trajectory data is imported into a GMM in MatLab software. Trajectory information is then generated by training the model and retrieving generalised trajectory data through Gaussian Mixture Regression (GMR). In particular, a GMM model with N components can be defined for a data set represented by λ by the probability density function in (1).

$$P(\lambda) = \sum_{n=1}^{N} P(N)P(\lambda|N) \tag{1}$$

$P(N)$ is a priori and $P(\lambda|N)$ is the conditional probability density function. The GMMs are then trained with an Expectation Maximisation (EM) algorithm to estimate the maximum log-likelihood of the GMM parameters. The optimal number of components $N\,(1\,to\,10)$ of the GMM is found based on the Bayesian Information Criterion (BIC) in (2).

$$BIC = -\sum_{j=1}^{K} log(P(\varsigma_j)) + \frac{n_p}{2} log(K) \tag{2}$$

ς_j is the trajectory datapoints, K is the number of points for one trajectory and n_p is the number parameters for a mixture of N components. The model with the highest BIC score has been selected. The optimal trajectory of the catheter tip by GMR can estimate the expected catheter tip trajectory, where the expected distribution of the catheter trajectory within the phantom can be defined as in (3).

$$\omega_n = \frac{P(\lambda|n)}{\sum_{n=1}^{N} P(\lambda|i)} \tag{3}$$

ω_n represents the expected distribution of catheter tips at different time steps. Trajectory data sets of catheter advancements and pullbacks after the GMM and GMR will then return new optimised trajectories for both procedures.

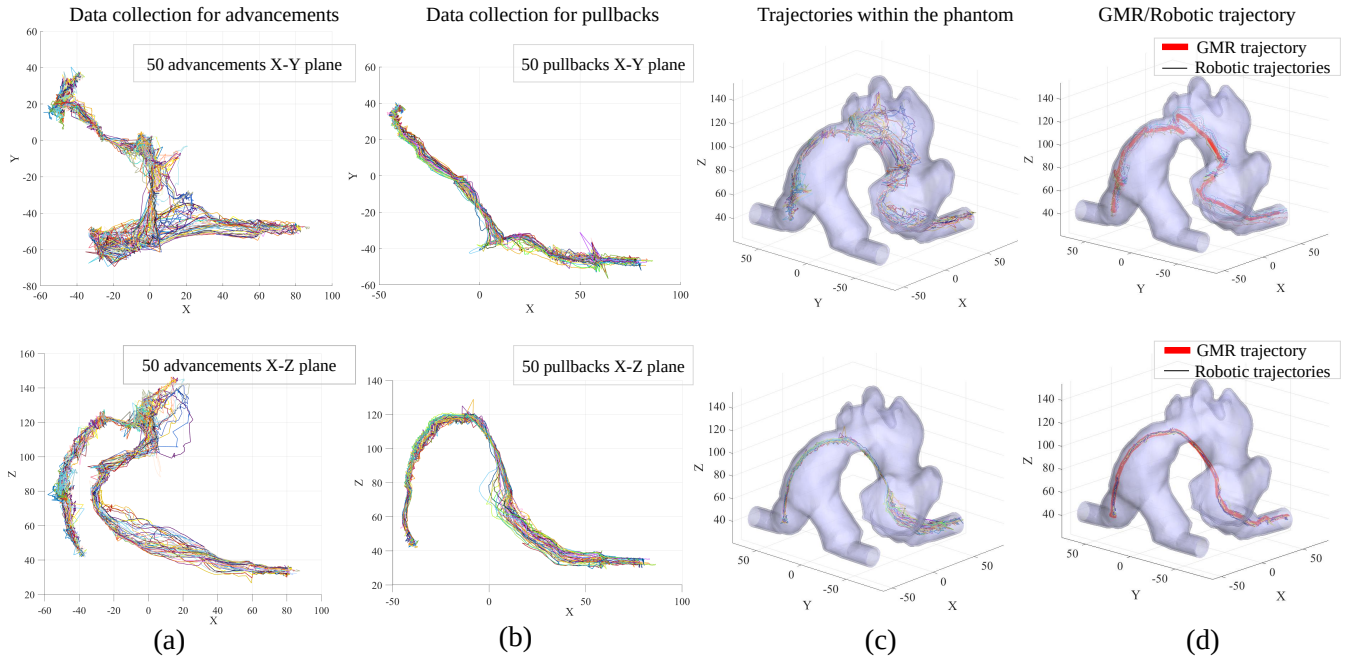

Fig. 3. Catheter tip trajectories: (a) 50 repetitions of catheter advancements shown in the $x-y$ plane (top) and $x-z$ plane (bottom) when robotically operated, (c) 50 repetitions of catheter pullbacks shown in the $x-y$ plane (top) and $x-z$ plane (bottom) when robotically operated, (c) 50 repetitions of catheter advancements (top) and pullbacks (bottom) shown inside the phantom CAD model when robotically operated, (d) 20 repetitions of the LfD based GMR generated trajectory (red colour) and executed robot-assisted trajectory of the catheter tip when advanced (top) and pulled back (bottom) inside the phantom CAD model

D. Experimental results of the GMR generated trajectory and discussion

Experiments have been carried out to demonstrate that the generated trajectories using the method in Section III-C can be autonomously executed by our catheterization robot. In Fig. 3(d) the red curve shows the resulting trajectory plotted inside the CAD model of the pulmonary artery phantom for the catheter advancement (top) and pullback (bottom). This trajectory has been given as input to our 2-DoF catheterization robot. The robot then steered the tip of the catheter through the phantom along the generated trajectory. The magnetic sensor recorded the position of the catheter tip which is plotted in blue colour for the advancement (top) and pullback (bottom) procedure.

For the advancement trajectory in Fig. 3(b) (top), the executed trajectory by the catheterization robot deviates from the LfD based GMM generated trajectory in some sections. The largest deviations can be observed before entering the RA and the PA. These errors might occur as the catheter will need to follow a larger bending trajectory with only being able to either translate or rotate the tip. With regards to the results of the experiments however, it can be seen that the robot-assisted pullback trajectory (Fig. 3(d) (bottom)) is similar to the trajectory generated by the LfD based GMM algorithm.

In Table I, the average and fastest time required for the advancement and pullback of the catheter for three different type of modes (i.e., manual hand-held, teleoperated robotic and autonomous robotic mode) is reported. From the summarised data, it can be concluded that the times required for the manual hand-held procedures are always larger compared to the procedures performed by the robot. For the advancement of the catheter, involving the 2-DoF robot is at least 15% quicker (about $5\,\mathrm{s}$) quicker than the manual procedure. Comparing the teleoperated with the autonomous procedure, it can be seen that the advancement of the catheter can be accelerated by about 15% (about $4\,\mathrm{s}$) in autonomous mode. This trend can also be seen in the times for the pullback of the catheter. However, the time differences are less significant (less than $1\,\mathrm{s}$) due to the simpler procedure compared to advancing the robot from the IVC to the PA.

IV. CONCLUSIONS

This paper presents a LfD based GMM for a robot trajectory optimisation during right heart catheterization using 50 repetitions of catheter advancements and pullbacks. We integrated the generated trajectory into our 2-DoF MR-compatible interventional robot steering a PA catheter from the IVC, through the RA and the RV into the PA where pressure measurements are conventionally made. The results of the experiment supports the feasibility of using the LfD based on GMM and GMR for trajectory optimisation of the catheter operated by robot. In addition, it can be concluded

TABLE I

TIME COMPARISON OF DIFFERENT MODES OF PERFORMING THE INTERVENTION IN THE PULMONARY ARTERY PHANTOM

Evaluation criteria	**Mode of procedure**		
	Manual hand-held	***Teleoperated robotic***	***Autonomous robotic***
Average time for advancement	32.5s	27.5s	23.7s
Fastest time for advancement	30.5s	25.6s	21.7s
Average time for pullback	10.7s	9.8s	8.9s
Fastest time for pullback	9.6s	8.4s	8.1s

that procedures performed by the robot in a teleoperated or autonomous mode requires significantly less time compared to manual hand-held procedures.

It is worth mentioning that the experiments were conducted in a non-pulsating phantom environment. Future work will enhance the phantom environment connecting a pulsatile blood pump (Harvard Apparatus, The USA) to the phantom. The pulsatile blood pump truly simulates the pumping action of the heart. Considering the variability of the shape of the pulmonary artery in real cases, 5 patient-specific shapes for the PA phantoms will be tested to evaluate the feasibility and applicability of the robotic system. In addition, we will collaborate with clinical cardiologists and clinicians to collect trajectory data and feedback from robotic operation to improve the autonomy of the robot.

REFERENCES

[1] "Cardiovascular Diseases", World Health Organization, 2020. [Online]. Available: https://www.who.int/health topics/cardiovascular diseases, accessed September 2022.

[2] V. Fuster, B.B. Kelly, "Rajesh Vedanta Global Cardiovascular Health: Urgent Need for an Intersectoral Approach", *Journal of the American College of Cardiology*, pp. 1208-1210, 2011.

[3] Y. Manda, K. Baradhi, "Cardiac Catheterization Risks and Complications", *StatPearls Publishing, Treasure Island (FL)*, 2021.

[4] J. Jayender, M. Azizian, RV Patel, "Autonomous Image-Guided Robot-Assisted Active Catheter Insertion", *IEEE Transactions on Robotics*, vol. 24, no. 4, pp. 858-871, 2008.

[5] S.B. Kesner, R.D. Howe. "Force Control of Flexible Catheter Robots for Beating Heart Surgery", *IEEE International Conference on Robotics and Automation*, pp. 1589-1594, 2011.

[6] D. Kundrat, G. Dagnino, T.M.Y. Kwok, M.E.M.K. Abdelaziz, W. Chi, A. Nguyen, C. Riga, G.-Z. Yang, "An MR-Safe Endovascular Robotic Platform: Design, Control, and Ex-Vivo Evaluation", in *IEEE Transactions on Biomedical Engineering*, vol. 68, no. 10, pp. 3110-3121, 2021.

[7] M.A. Tavallaei, Y. Thakur, S. Haider, M. Drangova, "A Magnetic-Resonance-Imaging-Compatible Remote Catheter Navigation System", in *IEEE Transactions on Biomedical Engineering*, vol. 60, no. 4, pp. 899-905, 2013.

[8] M.A. Tavallaei, M.K. Lavdas, D. Gelman, M. Drangova, "Magnetic resonance imaging compatible remote catheter navigation system with 3 degrees of freedom", *International Journal of CARS*, vol. 11, pp. 1537–1545, 2016.

[9] A. Attanasio, B. Scaglioni, E. De Momi, P. Fiorini, P. Valdastri, "Autonomy in Surgical", in *Annual Review of Control, Robotics, and Autonomous Systems*, vol. 4, pp. 651-679, 2020.

[10] S. Calinon, F. Guenter, A. Billard, "On Learning, Representing, and Generalizing a Task in a Humanoid Robot", in *IEEE Transactions on Systems, Man, and Cybernetics, Part B (Cybernetics)*, vol. 37, no. 2, pp. 286-298, 2007.

[11] Y.-Y. Tsai, B. Xiao, E. Johns, G.-Z. Yang, "Constrained-Space Optimization and Reinforcement Learning for Complex Tasks", in *IEEE Robotics and Automation Letters*, vol. 5, no. 2, pp. 683-690, 2020.

[12] I. Andras, E. Mazzone, F.W.B. van Leeuwen, "Artificial intelligence and robotics: a combination that is changing the operating room", *World Journal of Urology*, vol. 38, pp. 2359–2366, 2020.

[13] W. Chi, G. Dagnino, T.M.Y. Kwok, A. Nguyen, D. Kundrat, M.E.M.K. Abdelaziz, C. Riga, C. Bicknell, G.-Z. Yang, "Collaborative Robot-Assisted Endovascular Catheterization with Generative Adversarial Imitation Learning," *IEEE International Conference on Robotics and Automation*, pp. 2414-2420, 2020.

[14] W. Chi, J. Liu, H. Rafii-Tari, R. Celia, B. Colin, G.-Z. Yang, "Learning-based endovascular navigation through the use of non-rigid registration for collaborative robotic catheterization", *International Journal of Computer Assisted Radiology and Surgery*. vol. 13, pp. 855–864, 2018.

[15] C. Ye, J. Yang, H. Ding, "Bagging for Gaussian mixture regression in robot learning from demonstration", *Journal of Intelligent Manufacturing*, vol.33, pp. 867–879, 2022.

[16] J. Woo, H.-S. Song, H-J. Cha, B-J. Yi "Advantage of Steerable Catheter and Haptic Feedback for a 5- DOF Vascular Intervention Robot System", *Applied Sciences*. vol. 9, no.20, pp. 4305, 2019.

[17] K.H. Lee Lee, K.C.D. Fu, Z-Y. Guo, Ziyan, Z-Y. Dong, Martin C.W. Leong, C.L. Lee, A.P.W. Lee, W.Luk, K-W. Kwok, "MR Safe Robotic Manipulator for MRI-Guided Intracardiac Catheterization", in *IEEE/ASME Transactions on Mechatronics*, vol. 23, no. 2, pp. 586-595, 2018.

[18] M.E.M.K. Abdelaziz, D. Kundrat, M. Pupillo, G. Dagnino, T. Kwok, W. Chi, G. Vincent, F. Siepel, C. Riga, S. Stramigioli, G-Z. Yang, "Toward a Versatile Robotic Platform for Fluoroscopy and MRI-Guided Endovascular Interventions: A Pre-Clinical Study", *IEEE/RSJ International Conference on Intelligent Robots and Systems (IROS)*, pp. 5411-5418, 2019.

[19] H. Su, A. Mariani, S.E. Ovur, A. Menciassi, G. Ferrigno, E. De Momi, "Toward Teaching by Demonstration for Robot-Assisted Minimally Invasive Surgery", in *IEEE Transactions on Automation Science and Engineering*, vol. 18, no. 2, pp. 484-494, 2021.

[20] C.M. Heunis, Y. P. Wotte, J. Sikorski, G.P. Furtado, S. Misra, "The ARMM System - Autonomous Steering of Magnetically-Actuated Catheters: Towards Endovascular Applications", in *IEEE Robotics and Automation Letters*, vol. 5, no. 2, pp. 705-712, 2020.

[21] G.R. Sutherland, S. Lama, L. S. Gan, S. Wolfsberger, K. Zareinia, "Merging machines with microsurgery: Clinical experience with neuroArm", *Journal of Neurosurgery*, vol. 118, no. 3, pp. 521–529, 2013.

[22] F. Frank, A. Paraschos, P. van der Smagt, B. Cseke, "Constrained Probabilistic Movement Primitives for Robot Trajectory Adaptation", in *IEEE Transactions on Robotics*, vol. 38, no. 4, pp. 2276-2294, 2022.

[23] Y. Wu, F. Zhao, T. Tao, A. Ajoudani, "A Framework for Autonomous Impedance Regulation of Robots Based on Imitation Learning and Optimal Control", in *IEEE Robotics and Automation Letters*, vol. 6, no. 1, pp. 127-134, 2021.

[24] Z. Jin, A. Liu, W.-A. Zhang, L. Yu, "An Optimal Variable Impedance Control With Consideration of the Stability", in *IEEE Robotics and Automation Letters*, vol. 7, no. 2, pp. 1737-1744, 2022.

[25] S. Guo, J. Cui, Y. Zhao, Y. Wang, Y. Ma, W. Gao, G.Mao, "Shunming Hong Machine learning–based operation skills assessment with vascular difficulty index for vascular intervention surgery", *Medical, Biological Engineering and Computing*, Vol. 58, pp. 1707–1721, 2020.

[26] P. Sharma, A. Gupta, D. Ghosh, V. Honkote, G. Nandakumar, D. Ghose, "PG-RRT: A Gaussian Mixture Model Driven, Kinematically Constrained Bi-directional RRT for Robot Path Planning", *2021 IEEE/RSJ International Conference on Intelligent Robots and Systems*, pp. 3666-3673, 2021.

[27] L. Wang, S. Jia, G. Wang, Likun Wang, T.S.R. Alison, "Enhancing learning capabilities of movement primitives under distributed probabilistic framework for flexible assembly tasks", *Neural Computing and Applications*, 2021.